



Article

Study on the Characterization and Degradation Pattern of Circular RNA Vaccines Using an HPLC Method

Feiran Cheng^{1,2,3,4,5,†}, Ji Li^{6,†}, Chaoying Hu^{1,2,3,4,5}, Yu Bai¹, Jianyang Liu¹, Dong Liu¹, Qian He^{1,2,3,4,5}, Qiuhe Jin⁶, Qunying Mao^{1,2,3,4,5,*}, Zhenglun Liang^{1,2,3,4,5} and Miao Xu^{1,2,3,4,5,*}

¹ Institute of Biological Products, Division of Hepatitis and Enterovirus Vaccines, National Institutes for Food and Drug Control, Beijing 102629, China; 18249518559@163.com (F.C.); huchaoying2000@163.com (C.H.); blbaiyu@163.com (Y.B.); liujianyang123@126.com (J.L.); ld_nifdc@163.com (D.L.); hq5740@126.com (Q.H.); lzhenlun@126.com (Z.L.)

² Key Laboratory of Research on Quality and Standardization of Biotech Products, Beijing 102629, China

³ Evaluation of Biological Products, Beijing 102629, China

⁴ State Key Laboratory of Drug Regulatory Science, Institute of Biological Products, National Institutes for Food and Drug Control, Beijing 102629, China

⁵ Research Units of Innovative Vaccine Quality Evaluation and Standardization, Chinese Academy of Medical Sciences, Beijing 102629, China

⁶ Vazyme Biotech Co., Ltd., Nanjing 210089, China; lij@vazyme.com (J.L.); jinqiuhe@vazyme.com (Q.J.)

* Correspondence: maoqunying@126.com (Q.M.); xumiaobj@126.com (M.X.)

† These authors contributed equally to this work.

Abstract: Circular RNA (circRNA) vaccines have attracted increasing attention due to their stable closed-loop structures and persistent protein expression ability. During the synthesis process, nicked circRNAs with similar molecular weights to those of circRNAs are generated. Analytical techniques based on differences in molecular weight, such as capillary electrophoresis, struggle to distinguish between circRNAs and nicked circRNAs. The characteristic degradation products of circRNAs and their biological activities remain unclear. Therefore, developing methods to identify target circRNAs and non-target components and investigating degradation patterns will be beneficial to gaining an in-depth understanding of the properties and quality control of circRNAs vaccines. The reversed-phase HPLC (RP-HPLC) method was established for identification of target circRNAs, product-related substances, and impurities. Subsequently, we investigated the degradation patterns of circRNAs under thermal acceleration conditions and performed biological analysis of degradation products and linear precursors. Here, RP-HPLC method effectively identified circRNAs and nicked circRNAs. With thermal acceleration, circRNAs exhibited a “circular → nicked circRNAs → degradation products” degradation pattern. Biological analysis revealed that the immunogenicity of degradation products significantly decreased, whereas linear precursors did not possess immunogenicity. Thus, our established RP-HPLC method can be used for purity analysis of circRNA vaccines, which contributes to the quality control of circRNA vaccines and promoting the development of circRNA technology.

Keywords: circular RNAs; RNA vaccines; purity; degradation pattern; RP-HPLC



Citation: Cheng, F.; Li, J.; Hu, C.; Bai, Y.; Liu, J.; Liu, D.; He, Q.; Jin, Q.; Mao, Q.; Liang, Z.; et al. Study on the Characterization and Degradation Pattern of Circular RNA Vaccines Using an HPLC Method. *Chemosensors* **2024**, *12*, 120. <https://doi.org/10.3390/chemosensors12070120>

Academic Editor: Núria Serrano

Received: 30 April 2024

Revised: 22 May 2024

Accepted: 17 June 2024

Published: 1 July 2024



Copyright: © 2024 by the authors. Licensee MDPI, Basel, Switzerland. This article is an open access article distributed under the terms and conditions of the Creative Commons Attribution (CC BY) license (<https://creativecommons.org/licenses/by/4.0/>).

1. Introduction

The successful application of SARS-CoV-2 mRNA vaccines in recent years has sparked immense interest in RNA-based therapies [1]. As a unique class of RNA molecules, circular RNAs (circRNAs) have been identified for over 40 years [2,3]. CircRNAs are covalently closed, single-stranded RNA formed by back-splicing of precursor mRNAs [4–7]. During the splicing process, a downstream splice donor site is covalently linked to an upstream splice acceptor site [8–10]. Compared with linear mRNA, circRNA molecules possess a closed-loop structure that protects them from exonuclease-mediated degradation and thus confers high stability [11]. CircRNAs also exhibit a longer half-life in mammalian cells [9]. The existence of differences in production and structure between circRNAs and linear

mRNAs suggests that circRNAs may possess unique cellular functions and potential for biological applications [12].

CircRNAs have recently attracted widespread attention due to their key roles in gene delivery, protein production, and vaccine development [12–15]. In particular, circRNA vaccines have demonstrated immense potential for applications in infectious disease prevention and cancer treatment [16,17]. Due to the importance of ensuring the safety and effectiveness of circRNA vaccines, quality control of such vaccines has become a popular topic in research on circRNAs. During the *in vitro* synthesis process of circRNAs, substances such as nicked circRNAs, linear precursors, and introns are included in addition to target circRNAs [18]. Researchers have developed various physicochemical analytical methods to characterize the *in vitro* transcription (IVT) products of circRNAs [13,18]. For instance, capillary electrophoresis (CE) and gel electrophoresis are convenient and widely used methods for analyzing circRNAs. However, they are incapable of identifying and separating circRNAs and nicked circRNAs due to the unique structures and similar molecular weights of the two types of RNAs. Certain researchers have attempted to develop HPLC-based analytical methods, but these methods have yet to achieve successful identification and separation of circRNAs and nicked circRNAs [19]. Therefore, there is a need to develop test methods that can effectively identify circRNAs and nicked circRNAs to provide a basis for improving purity analyses of circRNA vaccines. In addition, despite the higher stability of the closed-loop structures of circRNAs compared with linear mRNAs, circRNAs can still be cleaved and degraded by ribonucleases (RNases). CircRNAs may be degraded within cells through various enzymatic pathways [20]. However, the characteristic degradation products of circRNAs and their biological functions remain unclear. Furthermore, the World Health Organization (WHO) and drug regulatory agencies such as the United States Food and Drug Administration (US FDA), European Medicines Agency, and Center for Drug Evaluation have not yet issued documents for the regulation and guidance of quality control of circRNA vaccines. In contrast, greater progress has been made in the optimization of design strategies and analytical methods for linear mRNA vaccines. This has led to significant improvements in the immunogenicity and characterization analysis of linear mRNA vaccines [21–26]. In addition, linear mRNA vaccines for coronavirus disease 2019 (COVID-19) have already received marketing approval [27], and recent research has provided insights into the degradation mechanisms of mRNA molecules in linear mRNA vaccines that have undergone thermal acceleration treatment [28].

Therefore, research on methods to identify circRNAs, product-related substances, and impurities, and to elucidate the degradation patterns of circRNAs and biological activities of degradation products, is of great significance in improving methods for circRNA vaccine purity analysis and gaining an in-depth understanding of the quality characteristics of circRNA vaccines. The RP-HPLC method established in this study achieved effective identification of target circRNA components, degradation products, and linear precursors. Through thermal acceleration, it was observed that the circRNAs exhibited a “circular→nicked circular→degradation products” degradation pattern. Our findings can hopefully guide the quality control and technical evaluation of circRNA vaccines, thereby promoting high-quality circRNA vaccine development.

2. Materials and Methods

2.1. Plasmids, IVT Templates, and RNA Synthesis

The Enhanced Green Fluorescent Protein (EGFP) plasmid was purchased from GenScript and linearized using a BsaI restriction enzyme (Vazyme). The circRNA precursor was synthesized using the T7 High Yield RNA Transcription Kit (Vazyme) with the linearized plasmids. The circRNA products were synthesized via a one-step reaction with the T7 High Yield RNA Transcription Kit (Vazyme); then, the reaction was incubated at 48 °C for 2 h to catalyze the cyclization of circRNAs. After the reaction, the remaining linearized plasmids were digested by DNase I (Vazyme), and the circRNAs were directly purified by VAHTS RNA Clean Beads (Vazyme).

2.2. RNase R Cleavage Assay

The RNA was heated at 65 °C for 3 min before being cooled on ice. The RNase R (Vazyme) was then added and incubated at 37 °C for 30 min. The reactions were stopped through incubation at 70 °C for 10 min, and RNAs were purified by VAHTS RNA Clean Beads (Vazyme) for capillary electrophoresis analysis.

2.3. CircRNA Purification and Analysis by HPLC

RNA was run through a 7.8×300 -mm size-exclusion column with a particle size of 5 μm and a pore size of 1000 Å (Sepax Technologies, Newark, DE, USA) on a Vanquish Flex UHPLC (Thermo, Waltham, MA, USA). RNA was run in an RNase-free phosphate buffer (225 mM NaH_2PO_4 , 225 mM Na_2HPO_4 , pH = 7.0) at a flow rate of 0.3 mL/min. RNA was detected through UV absorbance at 260 nm. RNA was also analyzed by reversed-phase high-performance liquid chromatography using a Thermo Vanquish Core HPLC system (Thermo) with a UV detector and an AcclaimTM 300 C18 column (AcclaimTM 300 C18, 3 μm , 150×4.6 mm) (Thermo) held at 55 °C. Chromatography was performed at a flow rate of 0.3 mL/min. Mobile phase A consisted of 100 mM TEAA. Mobile phase B consisted of 5% 100 mM TEAA and 95% acetonitrile. RNA was monitored by UV absorbance at 260 nm. Circular RNA, nicked RNA, and aggregations were purified individually by manual collection from multiple runs using VAHTS RNA Clean Beads, and pooled to generate sufficient material for downstream experiments.

2.4. Capillary Electrophoresis

The characterization of the circRNA sample was analyzed by capillary electrophoresis (Qsep 100, Bioptic Inc., Changzhou, China). In summary, before the experiment, the circRNAs RNA sample was heated at 70 °C for pre-treatment, and then placed on ice. After cooling, the 20ug circRNA sample was placed on the sample stage and analyzed according to the instrument operating instructions.

2.5. Cell Culture and Transfections

A human pulmonary carcinoma cell line (A549) and HEK293 cells were cultured at 37 °C and 5% CO_2 in Dulbecco's Modified Eagle Medium (Gibco, Waltham, MA, USA) supplemented with 10% fetal bovine serum (FBS, Gibco) and 1% penicillin/streptomycin. The circRNAs (2000 ng) were reverse transfected into 3×10^4 A549 cells per well in 24-well plate using the TransIT-mRNA Transfection Kit (Mirus, Madison, WI, USA) following the manufacturer's instructions. EGFP protein expression was detected by flow cytometry (Agilent, Santa Clara, CA, USA) and confocal laser scanning microscopy (Olympus, Hachioji, Japan) after transfection. For the reporter data in our study, reporter cells purchased from InvivoGene (San Diego, CA, USA) are HEK293-derived cells that stably express the Lucia luciferase secreted reporter gene. This reporter gene is under the control of the interferon (IFN)-inducible promoter which comprises the IFN-stimulated gene 54 promoter enhanced by multimeric IFN-stimulated response elements. Fluorescence intensity was measured in wild-type and pattern recognition receptors (PRR)-knockout reporter cells after transfection with 2000 ng RNA. The activity of the reporter gene was measured by mixing the supernatant and the fluorogenic substrate (QUANTI-Luc, rep-qlcg1, InvivoGen, San Diego, CA, USA), and luminescence was detected quickly afterward (EnVision 2105, PerkinElmer, Waltham, MA, USA).

2.6. Animal Study

Specific pathogen-free BALB/c mice were provided and maintained by the Chinese National Institutes of Food and Drug Control. For in vivo studies, BALB/c mice (6–8 weeks old, 18–20 g) were randomly and equally assigned to eight groups including circular, nicked, aggregation, degradation products, unpurified circRNAs, precursor, empty LNP, and phosphate buffer solution (PBS). Mice in experimental groups were immunized with 10 μg circRNA by intramuscular injection. Negative control groups were treated

with empty lipid nanoparticles (LNPs) or phosphate-buffered saline. At 12 h and 14 days after immunization, blood was collected for subsequent multiple-cytokine and IgG binding antibody titer detection, respectively.

2.7. Serum Cytokine Detection

Mouse serum inflammatory cytokines were detected by a V-PLEX Proinflammatory Panel 1 (mouse) Kit (MesoScale Discovery). The serum sample was diluted twice and cytokines testing performed under the guidance of the instrument manual. At the same time, standard samples were tested to ensure the accuracy of the experiment. All sample plates were analyzed by MSD Reader and Discovery Workbench (v4.0.13).

2.8. Enzyme-Linked Immunosorbent Assay (ELISA)

ELISA was used to measure IgG antibody titers in the mouse serum. Levels of serum IgG binding antibodies directed against the EGFP antigen were detected by ELISA. Plates with 96 wells were pre-treated with 1 µg/mL EGFP protein at 4 °C to bind the antigen. Afterwards, the plates were washed to remove unbound EGFP protein and blocked with 10% FBS diluted by PBST. Then the serum was diluted ten times serially in the plates and the IgG antibodies were detected under the incubation of goat anti-mouse IgG (HRP-labeled) (ZSGB-BIO) and substrate (Wantai BioPharm, Beijing, China) at dual wavelength. Lastly, the IgG titer results of the samples were analyzed according to their absorbance value which reached 2.1 times higher than negative control.

2.9. Statistical Significance

Statistical analyses were performed using GraphPad Prism 8.0. Statistical analyses were performed between the two groups using Student's *t*-test and comparisons between multiple groups were analyzed using one-way analysis of variance. Statistical significance was defined as $p < 0.05$.

3. Results

3.1. Establishment and Validation of the RP-HPLC-Based circRNA Vaccine Purity Analytical Method

Regulatory agencies such as the WHO have promulgated a series of guidance documents for research on the quality control of RNA vaccines. In particular, the second edition of the draft guidelines *Analytical Procedures for mRNA Vaccine Quality* issued by the United States Pharmacopeia (USP) has proposed analytical methods that cover the full life cycle of linear mRNA vaccines. However, for circRNA vaccines, it is usually difficult to effectively distinguish between circRNAs and nicked circRNAs by RNA analytical methods commonly used in current research, such as CE. To enhance the robustness of analytical methods for circRNAs, we attempted to establish an analytical method suitable for circRNA vaccines by referring to the linear mRNA vaccine characterization methods stated in the second edition of the *Analytical Procedures for mRNA Vaccine Quality* issued by the USP, including CE, RP-HPLC, and size-exclusion HPLC (SEC-HPLC).

Based on in vitro transcribed principles of circRNAs, we synthesized EGFP-encoding circRNAs, nicked circRNAs, and linear precursors by adopting the group I intron self-splicing method (Figure 1A). CE could detect both the circRNAs and linear precursors but was unable to achieve baseline separation or distinguish between circRNAs and nicked circRNAs (Figure 1B).

To achieve the identification of circRNAs and nicked circRNAs, we performed chromatographic column screening and mobile phase optimization to develop an RP-HPLC method capable of effectively identifying circRNAs, nicked circRNAs, and linear precursors. The results indicated that baseline separation was achieved (Figure 1C). Based on the recommendations of the International Council for Harmonisation (ICH) Q2(R2) Guideline, we validated the specificity, quantitation limit, detection limit, and precision of the developed RP-HPLC method. The specificity test revealed that the solvent did not interfere with

RNA detection (Figure 1C). The detection limits of the RP-HPLC method for the circRNAs, nicked circRNAs, and linear precursors samples were 2.4, 1.7, and 1.7 ng/ μ L, respectively, and the quantitation limits were 7.1, 5, and 5 ng/ μ L, respectively. These limit ranges demonstrated the applicability of the developed method to future quality studies. Lastly, results of precision validation revealed that the relative standard deviation for the testing of multiple circRNA samples by different researchers was merely 0.6%. This indicates that the precision of the RP-HPLC method fulfilled the precision requirement (Table 1). Therefore, validation of the specificity, quantitation limit, detection limit, and precision indicated that the RP-HPLC method was highly applicable to the identification and analysis of circRNAs and nicked circRNAs.

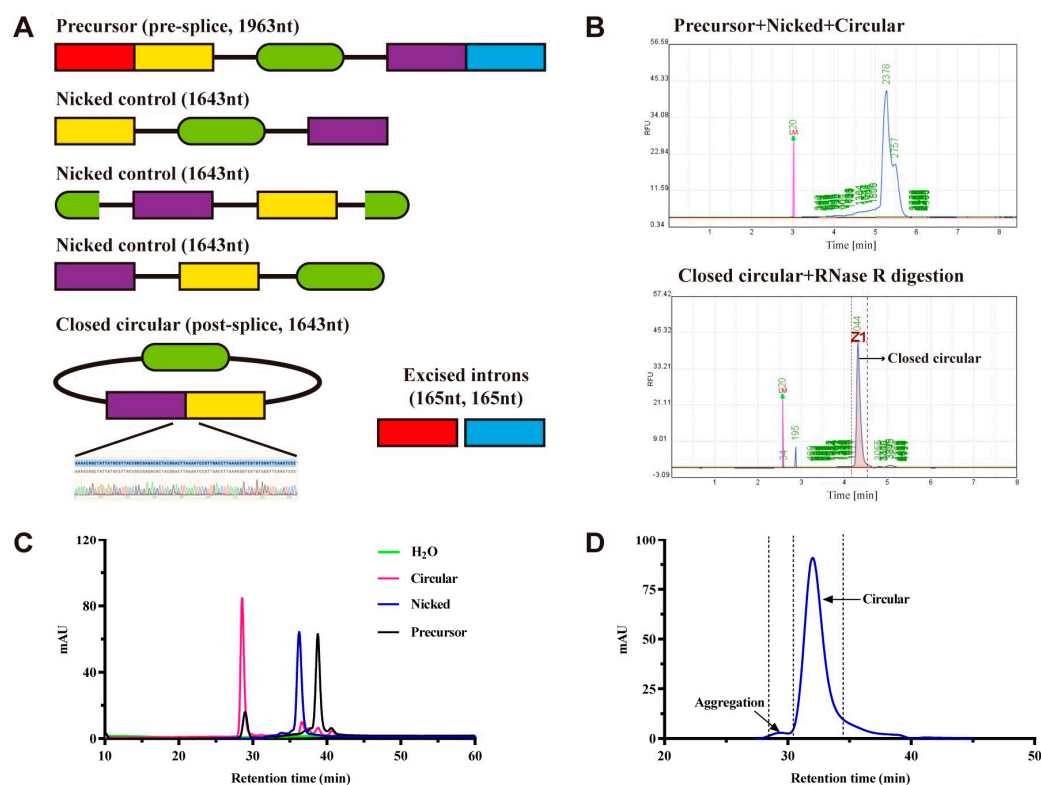


Figure 1. Establishment of high-performance liquid chromatography methods to confirm circular RNAs (circRNAs) identity. (A) Schematic and expected sizes of linear precursor, nicked control, and circular and excised introns. Nicked control RNA is splicing-incompetent as it lacks the full upstream and downstream introns necessary for splicing but retains remnant introns expected after splicing. CircRNA, nicked, and linear precursor (top), and circRNA purified by RNase R digestion measured by capillary electrophoresis (B), reverse-phase high-performance liquid chromatography (C), and size-exclusion chromatography (D), respectively.

A column temperature of 55 °C was selected for the RP-HPLC method, but it was unclear whether this temperature affected circRNA sample testing. Therefore, we investigated the stability of circRNA sample testing under the column temperature conditions. Compared with untreated circRNAs, a circRNA sample that had been incubated at 55 °C in the mobile phase for 30 min did not cause a significant change in the RP-HPLC results. This demonstrates that the column temperature and mobile phase of RP-HPLC did not interfere with circRNA sample testing (Figure S1).

Lastly, similar to the method for mRNA aggregate detection described in the USP guidelines [23], SEP-HPLC could detect and quantify circRNA aggregates (Figure 1D).

In summary, the RP-HPLC method could sensitively distinguish circRNAs, nicked circRNAs, and linear precursors, while SEP-HPLC could detect the aggregate structures of

circRNAs. These two HPLC methods enable considerable enhancement of circRNA testing and can be utilized for quality control analysis of circRNA vaccines.

Table 1. Overall precision of 12 samples prepared by two researchers.

Validation Researchers	Samples	Purity (%)	RSD (%)
Researcher 1	Sample-1	60.380	0.6
	Sample-2	59.190	
	Sample-3	59.390	
	Sample-4	59.840	
	Sample-5	58.910	
	Sample-6	59.490	
Researcher 2	Sample-1	59.580	
	Sample-2	59.750	
	Sample-3	59.650	
	Sample-4	59.700	
	Sample-5	59.840	
	Sample-6	59.320	

RSD: relative standard deviation.

3.2. Degradation Patterns of the circRNA Substance

Although the closed-loop structure of circRNAs makes them more stable than linear mRNAs, the degradation patterns of circRNAs remain unclear. We performed thermal acceleration treatment on the circRNA substance to determine the possible degradation products of circRNAs, establish pertinent identification and control methods, and analyze the biological characteristics of different related substances and impurities *in vivo* and *in vitro*, to provide a basis for devising quality control and evaluation methods for circRNA vaccines. The established RP-HPLC method described earlier demonstrated sensitive detection of circRNAs and nicked circRNAs, thereby providing technical support for exploring the degradation patterns of circRNAs under conditions of thermal acceleration.

First, the reaction products of IVT were purified by RP-HPLC to obtain the circRNA samples. Following the guiding principles for stability studies promulgated by the WHO and ICH [22,29,30], the circRNA samples were separately stored under different temperatures for thermal acceleration testing. The degradation of the circRNA samples was subsequently detected by HPLC to obtain and identify the degradation products of circRNAs.

RP-HPLC revealed that compared with the untreated group, the circRNA samples separately stored at 4 and 25 °C for one week and at 37 °C for one day had started to undergo circular degradation. With the generation of nicked circRNAs, the proportion of nicked circRNAs increased from approximately 15% to approximately 30%. Prolongation of storage time led to a further increase in the proportion of nicked circRNAs to about 40%. Subsequently, the proportion of nicked circRNAs decreased while the proportion of degradation products increased significantly from ~10% to ~60%. This was accompanied by a decrease in the purity of circRNAs to merely around 10%. The degradation products may have originated from further hydrolysis of the nicked circRNAs. Therefore, the RP-HPLC results indicated that under the thermal acceleration treatment conditions, the circRNAs exhibited a “circular→nicked→degradation products” degradation pattern (Figure 2A–C).

SEC-HPLC results revealed that the circRNA samples stored at 4 °C and 25 °C exhibited circular degradation accompanied by a decrease in aggregates and accumulation of degradation products (~9%→~80%) (Figure S2). However, the circRNA sample stored at 37 °C exhibited circular degradation accompanied by the accumulation of aggregates (~2%→~16%) and degradation products (~9%→~50%) (Figure S2). Therefore, SEC-HPLC results indicated that circRNAs exhibited degradation of circular RNAs and aggregates accompanied by formation of degradation products. Figure 2D summarizes the detailed test results obtained with RP-HPLC and SEC-HPLC. Results of CE could only indicate circRNA degradation and the formation of degradation products in the circRNA samples (Figure 2D).

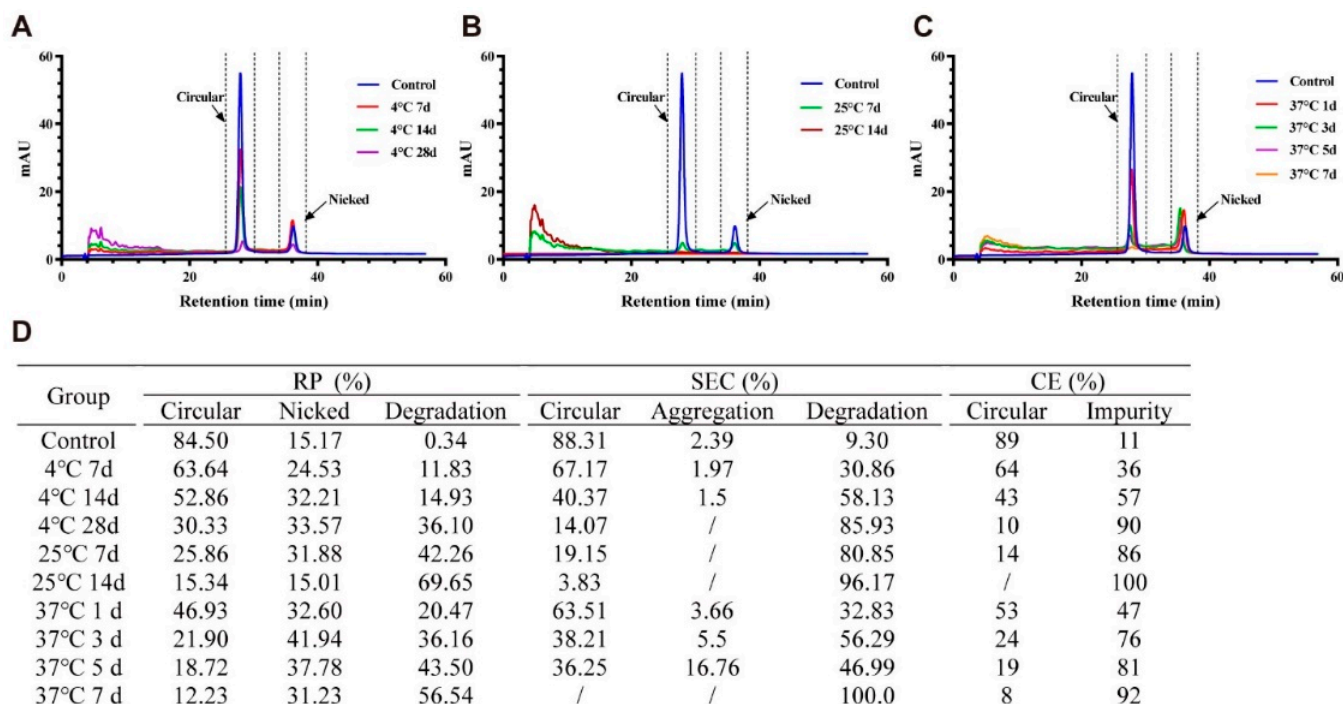


Figure 2. Stability studies of circular RNAs (circRNAs) under accelerated conditions. Degradation pattern of circRNAs measured by RP-HPLC at different time points at 4 °C (A), 25 °C (B), and 37 °C (C). CircRNAs stored at -20 °C serve as control. Summarized data of stability studies on circRNAs under different conditions measured by reversed-phase high-performance liquid chromatography (HPLC), size-exclusion HPLC, and capillary electrophoresis, respectively (D).

3.3. Expression Activities of Degradation Products of circRNAs and Linear Precursors

As described in the previous section, we observed that the circRNAs exhibited a “circular→nicked→degradation products” degradation pattern. However, the biological activities of degradation products of circRNAs remain unclear. To investigate the expression activities of the degradation products, we separately purified and collected the circRNAs, nicked circRNAs, aggregates, degradation products, and linear precursors. After collection, HPLC was used again for the characterization of the various circRNA components (Figure S3).

Subsequently, the expression activities of circRNAs and their degradation products were evaluated at the cellular level. A549 cells were separately transfected with the above circRNA species, and EGFP expression was measured by flow cytometry and confocal fluorescence microscopy. The results of flow cytometry indicated that circRNAs possessed sustained expression characteristics. EGFP expression levels increased continuously with the progression of time, as shown by a rise in fluorescence intensity from around 3×10^6 to around 7×10^6 . This also demonstrates that circRNAs had the advantage of stable expression compared with linear RNA (Figure 3A). The EGFP fluorescence intensities of the nicked circRNAs and aggregates were approximately 1/5 and 1/20 of that of the circRNAs, respectively. EGFP expression was not detected in the degradation products and linear precursors. The results of confocal fluorescence microscopy were also indicative of the same phenomenon (Figure 3B).

Therefore, the *in vitro* experiment demonstrated that the nicked circRNAs and aggregates exhibited a significant decrease in antigen expression activity levels compared with circRNAs, while the degradation products and linear precursors did not induce antigen expression.

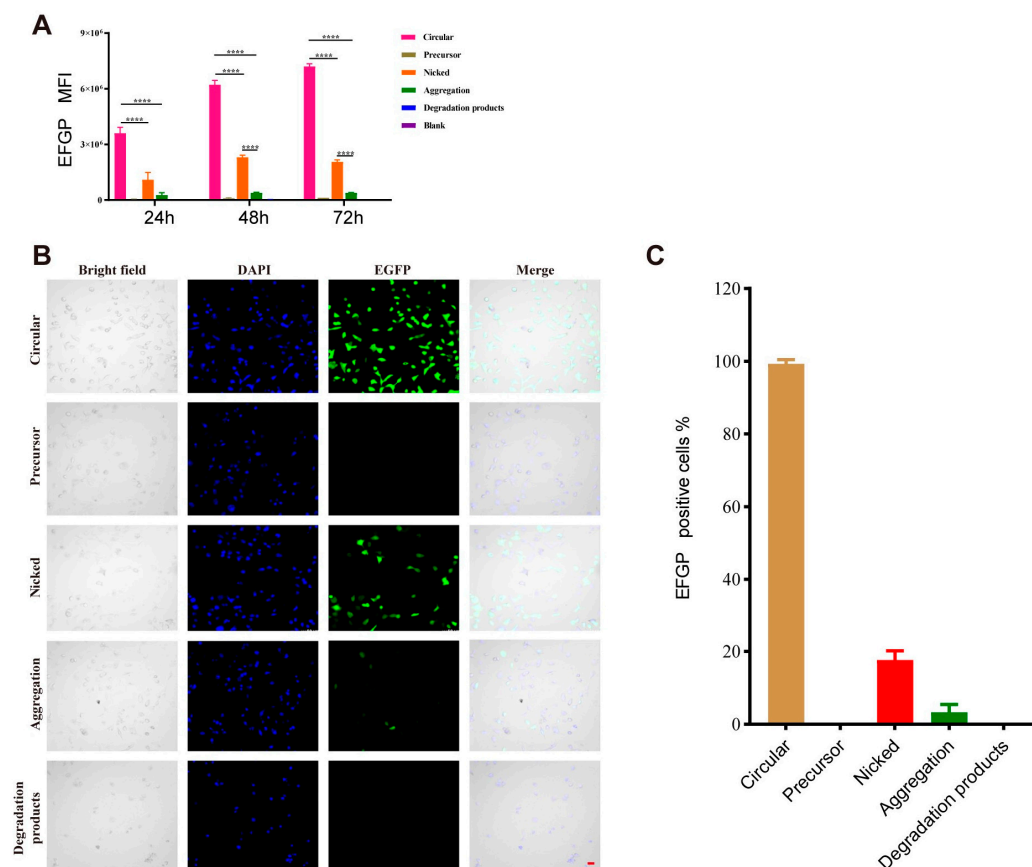


Figure 3. The antigen expression ability of circular RNA (circRNA) species in vitro. Mean fluorescence intensity of each group after transfection with circRNA species coding EGFP measured by flow cytometry (A). Bars represent means \pm standard deviation. **** $p < 0.0001$. Confocal microscope results are shown at 24 h after transfection (B) and the percentage of EGFP-positive cells for each group was calculated (C). (scale bar = 50 μ m).

3.4. In Vivo Immunogenicity and Safety of Degradation Products of circRNA Vaccines and Linear Precursors

The degradation pattern of circRNAs has been elucidated in the previous section. However, it remains unclear whether degradation products will affect the immunogenicity and safety of circRNA vaccines. LNPs were used for the encapsulation of unpurified circRNA obtained from IVT, purified circRNAs, nicked circRNAs, aggregates, degradation products, and linear precursors. The encapsulation efficiencies of the various groups exceeded 95% and the average particle size was around 80 nm (Figure 4A). Mice were immunized at a dose of 10 μ g/mouse by intramuscular injection, and the levels of inflammatory cytokines and anti-EGFP IgG binding antibody responses in the mice were measured. Figure 4B shows the detailed procedure of the animal experiment.

The serum inflammatory cytokine levels of the mice were measured 12 h after intramuscular injection. The results of the inflammatory cytokine analysis revealed an increase in the proinflammatory cytokine expression levels of the various experimental groups. In particular, IL-6 concentration reached approximately 3200–5700 pg/mL in the experimental groups, which was significantly higher than the levels measured in the blank control and empty LNP groups (2 and 190 pg/mL, respectively). However, the expression levels of anti-inflammatory factors were similar among the experimental groups.

Antibody levels were measured by ELISA at 14 days after immunization. The results indicated that the unpurified circRNAs effectively induced specific anti-EGFP IgG binding antibodies against EGFP, with the geometric mean titer (GMT) being approximately 4×10^3 . In particular, the specific IgG antibody level induced by the purified circRNAs was signifi-

cantly higher than that of the unpurified circRNAs ($p < 0.0001$), with the GMT reaching around 1×10^4 (Figure 4C). The anti-EGFP IgG antibody levels of the nicked circRNAs and aggregates were significantly lower than those of the purified and unpurified circRNAs, being merely approximately 6×10^2 and 4×10^2 , respectively ($p < 0.0001$). Neither the degradation products nor linear precursors induced antibody responses against EGFP (Figure 4C).

The results of inflammatory cytokines and anti-EGFP IgG antibody detection collectively suggest that circRNAs, degradation products, and linear precursors induced strong inflammatory responses. However, the induced specific anti-EGFP IgG antibody levels differed significantly among different groups.

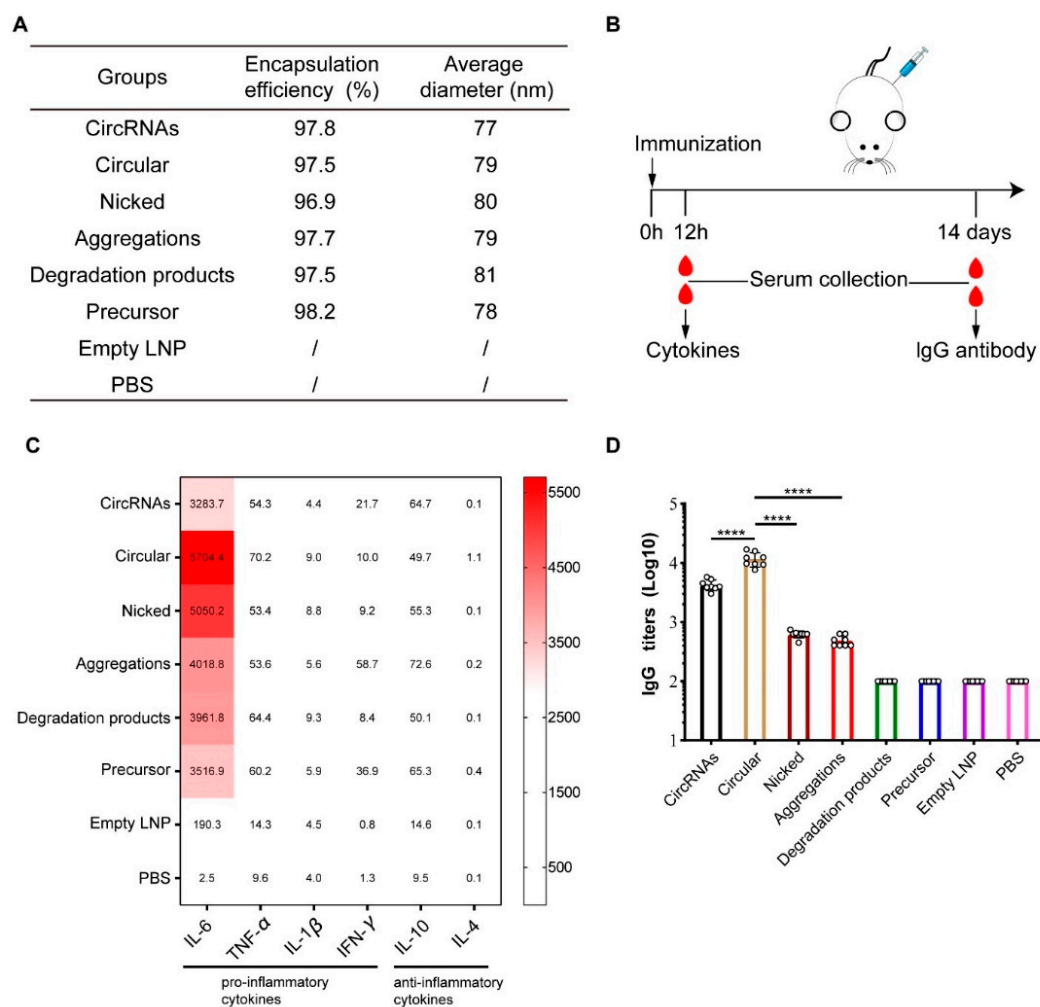


Figure 4. The induced immune response of circular RNA (circRNA) species in vivo. (A) Animal experimental groups and detailed sample parameters are represented. (B) An overview of the mice immunization and blood collection procedure. (C) Multiplex inflammatory cytokine analysis for each group; the concentration of each cytokine (pg/mL) is represented as a heatmap. (D) EGFP-specific anti-EGFP IgG binding antibody titers in mice 14 d post-first immunization. Bars represent geometric means \pm standard deviation. **** $p < 0.0001$. $n = 8$ for each group.

3.5. Activated Pattern Recognition Receptors of Degradation Products and Linear Precursors of circRNAs

The animal experiment described above revealed that circRNAs, degradation products, and linear precursors stimulated the release of high levels of inflammatory cytokines in mice. Inflammatory cytokine release is an immune response generated by the innate immune system through pattern recognition receptors and is aimed at recognizing and

resisting foreign pathogens [31–34]. Pattern recognition receptor reporter gene-expressing cells purchased by our laboratory were utilized to elucidate the molecular mechanisms by which inflammatory cytokine release was stimulated by circRNAs, degradation products, and linear precursors. The reporter cells were separately transfected with the circRNAs, degradation products, and linear precursors, and the empty transfection reagent was used as a control to investigate the types of pattern recognition receptors activated by the circRNAs, degradation products, and linear precursors.

After 24 h, the cells were collected for measurement of the expression levels of the fluorescence reporter gene. Compared with the high-intensity fluorescence signals stimulated by wild-type 293 cells, the fluorescence level induced by circRNAs was significantly reduced after retinoic acid-inducible gene I (RIG-I) knockout (KO). The intensities of fluorescence stimulated by the circRNA in Toll-like receptors (TLR) 3/8 KO cells, stimulated by aggregates and degradation products in TLR7/8 KO cells, and stimulated by linear precursors in TLR3 KO cells were also significantly lower (Figure 5A). These data indicate that the circRNAs could activate RIG-I, nicked circRNAs could activate TLR3 and TLR8, the degradation products and aggregates could activate TLR7 and TLR8, and the linear precursors could activate TLR3, thereby inducing an immune response.

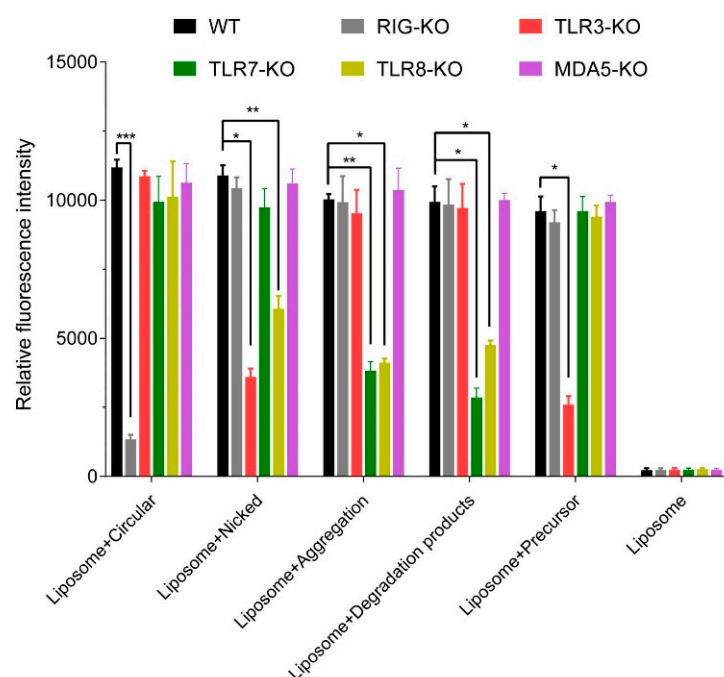


Figure 5. The activated pattern recognition receptors of circular RNAs and precursors. Relative fluorescence intensity in vitro 24 h after transfection in reporter cells. Data presented as means + SEM, $n = 3$, * $p < 0.05$. ** $p < 0.01$. *** $p < 0.001$.

4. Discussion

This study focused on the identification and characterization of circRNA vaccines and the investigation of their degradation patterns. IVT products of circRNAs not only consist of target circRNA but may also include nicked circRNAs, aggregates, and residual linear precursors. Commonly used analytical methods are incapable of effectively distinguishing between circRNAs and nicked circRNAs. The RP-HPLC method established and validated in this study demonstrated good discrimination and baseline separation of circRNAs and nicked circRNAs. This method also achieved excellent characterization of the degradation products of circRNAs and enabled the elucidation of the “circular → nicked → degradation products” degradation pattern of circRNAs under thermal acceleration conditions. The results of in vivo and in vitro experiments indicated that the degradation products of circRNAs had significantly lower biological activity levels but still elicited strong inflam-

matory immune responses. The reporter gene-expressing cell experiment further revealed that circRNAs could activate RIG-I, nicked circRNAs could activate TLR3 and TLR8, the degradation products and aggregates could activate TLR7 and TLR8, and the linear precursors could activate TLR3. These results explain the mechanisms by which inflammatory responses are generated. Therefore, this study has provided data and support for purity testing and quality control of linear precursors and degradation products during the development of circRNA vaccines.

The IVT process of circRNAs is relatively complex compared to that of linear mRNAs. Based on the IVT reaction of circRNAs and the data obtained in this study, a series of optimization strategies should be employed in the future development and design of circRNAs for the enhancement of purity to ensure the immunogenicity and safety of circRNA products. There are currently three main methods for the synthesis of circRNAs, namely group I intron, group II intron based permuted intron-exon (PIE) system, and ligation with T4 RNA ligases [35]. In particular, the PIE system possesses several advantages such as a rapid and convenient synthesis procedure, higher suitability for the circularization of longer sequence, and high product yield. Therefore, it has been widely used in laboratory research and circRNA vaccine development [13,36]. During the IVT process of circRNAs, optimization of parameters such as the circularization reaction temperature, buffer type, and type of T7 RNA polymerase can assist in downregulating the generation of nicked circRNAs and double-stranded RNA (dsRNA), thereby improving the purity of the produced circRNAs [18,37]. Furthermore, longer circRNA sequences are more prone to nicking [14]. Therefore, the shortening of circRNA sequence length is a key challenge in the development of circRNA vaccines. Screening for shorter internal ribosomal entry site-like sequences such as Kozak sequences and AU-rich sequences may help overcome these limitations [38]. Purification is a necessary step for the enhancement of circRNA vaccine purity. Residual linear precursors may activate innate immune responses, thereby affecting the immunogenicity and safety of circRNA vaccines [15,39–43]. For instance, RNase R digestion and SEP-HPLC can be used for the removal of linear precursors and intron fragments [14]. The RP-HPLC method established in this study effectively separated circRNAs, nicked circRNAs, and linear precursors. This indicates that our developed RP-HPLC method can also be used for the purification of circRNA vaccines.

The N1-methylpseudouridine (m1Ψ) modification is employed in two marketed COVID-19 mRNA vaccines. This modification not only considerably downregulates mRNA-induced innate immune responses but also elevates the expression levels of antigen proteins [24,44]. Currently, unmodified nucleotide raw materials are used in the production of circRNA vaccines. Upon entry into the body, circRNAs that have not undergone nucleotide modification can activate RIG-I. This activation induces an inflammatory cytokine response, which may affect the safety of circRNA vaccines [45–48]. The results of the animal experiment performed in this study also revealed that the unmodified circRNAs induced high expression levels of the inflammatory factor IL-6 (Figure 4D). However, the nicked circRNAs, degradation products, and linear precursors also stimulated the release of high IL-6 levels. Previous research has observed that nicked circRNAs can stimulate cells to release high IL-6 levels. Unlike the activation of RIG-I by circRNAs, nicked circRNAs can be recognized by the TLR3 and TLR8, leading to the release of inflammatory factors. Linear precursors can stimulate the release of IL-6 by cells through the activation of TLR3-mediated signaling pathways [15]. Some studies have reported that the degradation products of RNAs can serve as ligands for TLR7 and TLR8 [49,50]. The reporter gene-expressing cell experiment in this study revealed that the circRNAs, degradation products, and linear precursors could activate different pattern recognition receptors. Therefore, this study has also elucidated the molecular mechanisms of the inflammatory cytokine responses induced by circRNAs and their degradation products in animals. Although circRNAs and their degradation products and linear precursors possess significantly different abilities in inducing specific antibody responses, they are all capable of activating the pattern recognition receptors of the body, thereby inducing inflammatory cytokine responses.

The latest research has observed that the introduction of N6-methyladenosine (m6A) modifications can considerably reduce the inflammatory cytokine response levels of circRNAs [45]. In addition, m6A modifications do not affect the protein translation levels of circRNAs and may even enhance circRNA stability to a certain extent [51]. Interestingly, previous studies have demonstrated that m6A is the most abundant modification in naturally occurring mRNAs. It is present in approximately 0.5% of intracellular transcripts, including mRNAs, long non-coding RNAs, and circRNAs [52–55]. Based on these findings, research on the types of modifications in naturally occurring RNAs may provide new directions for the sequence design and optimization of circRNA vaccines, which will contribute to the enhancement of circRNA vaccine quality. In recent decades, the US FDA has introduced the quality-by-design approach in the development and quality control of new drugs. This concept can also provide guidance for the development, design, and quality control of circRNA vaccines.

Currently, there is a lack of guidance documents issued by regulatory agencies for quality control research on circRNA vaccines. Due to the unique synthesis process and reaction products of circRNAs, purity has become a critical quality attribute that requires close monitoring when performing quality control of circRNA vaccines. Commonly used analytical methods such as CE are incapable of effectively distinguishing between circRNAs and nicked circRNAs, thereby posing methodological requirements for purity analyses of circRNA vaccines. Validation of the RP-HPLC method established in this study has deemed it suitable for the identification and separation of circRNAs and nicked circRNAs. In the future, it can also be used in purity analysis and quality control studies of circRNA vaccines. Other novel circRNA identification methods besides HPLC, such as CE, should also be optimized to achieve the distinction between circRNAs and nicked circRNAs, providing further enhancement of analytical methodologies for circRNA vaccines. Lastly, we determined that the circRNA substance exhibited the “circular→nicked→degradation products” degradation pattern under conditions of thermal pressurization. Recent research on RNA vaccine products has observed that linear mRNAs can undergo adduction reactions with the degradation products of LNPs (e.g., aldehyde molecules), resulting in mRNA degradation and reduced expression activity levels [28]. However, the degradation patterns of circRNAs in LNP-containing circRNA vaccine products remain unclear.

5. Conclusions

Herein, we established an RP-HPLC method for the identification of circRNAs and nicked circRNAs, and elucidated the degradation pattern of the circRNA substance. However, these experimental findings were obtained from EGFP-encoding circRNAs and warrant further validation in marketed circRNA vaccines. Further research is also required to investigate the degradation patterns of circRNA molecules in circRNA vaccine products.

Supplementary Materials: The following supporting information can be downloaded at: <https://www.mdpi.com/article/10.3390/chemosensors12070120/s1>, Figure S1: Stability of circRNAs samples under column temperature measured by RP-HPLC; Figure S2: Stability studies of circRNAs samples treated under 4 °C (A), 25 °C (B) and 37 °C (C) measured by SEC-HPLC; Figure S3: Isolated closed-circular, linear precursor, nicked, aggregation, and degradation products from circRNAs were further confirmed by RP-HPLC and SEC-HPLC.

Author Contributions: Conceptualization, Q.J., Q.M., Z.L. and M.X.; methodology, F.C., D.L., J.L. (Jianyang Liu), Q.H. and Y.B.; formal analysis and investigation, F.C., J.L. (Ji Li) and C.H.; resources, Z.L.; data curation, F.C. and J.L. (Ji Li); writing—original draft preparation, F.C.; writing—review and editing, F.C. and Z.L.; visualization, Q.M.; supervision, Q.M., Z.L. and M.X.; project administration, Z.L. and M.X.; funding acquisition, Q.M. and M.X. All authors have read and agreed to the published version of the manuscript.

Funding: The author(s) declare that financial support was received for the research, authorship, and/or publication of this article. This study was supported by NIFDC Fund for Key Technology Research (GJJS-2022-1-1) (2023SKLDRS0119), National Key R&D Program (2023YFC2606004), the

Jiangsu Province Science and Technology Achievement Transformation Special Project (BA2023012), R&D Program of Guangzhou National Laboratory (Grant No. SRPG23-005), the Non-profit Central Research Institute Fund of the Chinese Academy of Medical Sciences (2023-PT350-01) and CAMS Innovation Fund for Medical Sciences (2021-I2M-5-005).

Institutional Review Board Statement: The study was conducted in accordance with the local legislation and institutional requirements and approved by the Institutional Animal Care and Use Committee of the National Institutes for Food and Drug Control [Approval number: 2024-B-008].

Informed Consent Statement: Not applicable.

Data Availability Statement: All data generated or analyzed and materials used during this study are included in this published article.

Conflicts of Interest: The authors Ji Li and Qiheng Jin are affiliated with Vazyme Biotech Co., Ltd. The remaining authors no conflict of interest.

References

- Liu, C.; Shi, Q.; Huang, X.; Koo, S.; Kong, N.; Tao, W. mRNA-based cancer therapeutics. *Nat. Rev. Cancer* **2023**, *23*, 526–543. [CrossRef]
- Arnberg, A.C.; Van Ommen, G.J.; Grivell, L.A.; Van Bruggen, E.F.; Borst, P. Some yeast mitochondrial RNAs are circular. *Cell* **1980**, *19*, 313–319. [CrossRef]
- Ngo, L.H.; Bert, A.G.; Dredge, B.K.; Williams, T.; Murphy, V.; Li, W.; Hamilton, W.B.; Carey, K.T.; Toubia, J.; Pillman, K.A.; et al. Nuclear export of circular RNA. *Nature* **2024**, *627*, 212–220. [CrossRef]
- Zhang, X.O.; Wang, H.B.; Zhang, Y.; Lu, X.; Chen, L.L.; Yang, L. Complementary sequence-mediated exon circularization. *Cell* **2014**, *159*, 134–147. [CrossRef]
- Starke, S.; Jost, I.; Rossbach, O.; Schneider, T.; Schreiner, S.; Hung, L.H.; Bindereif, A. Exon circularization requires canonical splice signals. *Cell Rep.* **2015**, *10*, 103–111. [CrossRef]
- Chen, L.L. The biogenesis and emerging roles of circular RNAs. *Nat. Rev. Mol. Cell Biol.* **2016**, *17*, 205–211. [CrossRef]
- Memczak, S.; Jens, M.; Elefsinioti, A.; Torti, F.; Krueger, J.; Rybak, A.; Maier, L.; Mackowiak, S.D.; Gregersen, L.H.; Munschauer, M.; et al. Circular RNAs are a large class of animal RNAs with regulatory potency. *Nature* **2013**, *495*, 333–338. [CrossRef]
- Nilsen, T.W.; Graveley, B.R. Expansion of the eukaryotic proteome by alternative splicing. *Nature* **2010**, *463*, 457–463. [CrossRef]
- Kristensen, L.S.; Andersen, M.S.; Stagsted, L.V.W.; Ebbesen, K.K.; Hansen, T.B.; Kjems, J. The biogenesis, biology and characterization of circular RNAs. *Nat. Rev. Genet.* **2019**, *20*, 675–691. [CrossRef]
- Sanger, H.L.; Klotz, G.; Riesner, D.; Gross, H.J.; Kleinschmidt, A.K. Viroids are single-stranded covalently closed circular RNA molecules existing as highly base-paired rod-like structures. *Proc. Natl. Acad. Sci. USA* **1976**, *73*, 3852–3856. [CrossRef]
- Enuka, Y.; Lauriola, M.; Feldman, M.E.; Sas-Chen, A.; Ulitsky, I.; Yarden, Y. Circular RNAs are long-lived and display only minimal early alterations in response to a growth factor. *Nucleic Acids Res.* **2016**, *44*, 1370–1383. [CrossRef]
- Chen, L.L. The expanding regulatory mechanisms and cellular functions of circular RNAs. *Nat. Rev. Mol. Cell Biol.* **2020**, *21*, 475–490. [CrossRef]
- Qu, L.; Yi, Z.; Shen, Y.; Lin, L.; Chen, F.; Xu, Y.; Wu, Z.; Tang, H.; Zhang, X.; Tian, F.; et al. Circular RNA vaccines against SARS-CoV-2 and emerging variants. *Cell* **2022**, *185*, 1728–1744.e16. [CrossRef]
- Wesselhoeft, R.A.; Kowalski, P.S.; Anderson, D.G. Engineering circular RNA for potent and stable translation in eukaryotic cells. *Nat. Commun.* **2018**, *9*, 2629. [CrossRef]
- Wesselhoeft, R.A.; Kowalski, P.S.; Parker-Hale, F.C.; Huang, Y.; Bisaria, N.; Anderson, D.G. RNA Circularization Diminishes Immunogenicity and Can Extend Translation Duration In Vivo. *Mol. Cell* **2019**, *74*, 508–520.e4. [CrossRef]
- Jin, Y.; Hou, C.; Li, Y.; Zheng, K.; Wang, C. mRNA Vaccine: How to Meet the Challenge of SARS-CoV-2. *Front. Immunol.* **2021**, *12*, 821538. [CrossRef]
- Duan, L.J.; Wang, Q.; Zhang, C.; Yang, D.X.; Zhang, X.Y. Potentialities and Challenges of mRNA Vaccine in Cancer Immunotherapy. *Front. Immunol.* **2022**, *13*, 923647. [CrossRef]
- Abe, B.T.; Wesselhoeft, R.A.; Chen, R.; Anderson, D.G.; Chang, H.Y. Circular RNA migration in agarose gel electrophoresis. *Mol. Cell* **2022**, *82*, 1768–1777.e3. [CrossRef]
- Lee, K.H.; Kim, S.; Song, J.; Han, S.R.; Kim, J.H.; Lee, S.W. Efficient circular RNA engineering by end-to-end self-targeting and splicing reaction using Tetrahymena group I intron ribozyme. *Mol. Ther. Nucleic Acids* **2023**, *33*, 587–598. [CrossRef]
- Ren, L.; Jiang, Q.; Mo, L.; Tan, L.; Dong, Q.; Meng, L.; Yang, N.; Li, G. Mechanisms of circular RNA degradation. *Commun. Biol.* **2022**, *5*, 1355. [CrossRef]
- USP. Analytical Procedures for mRNA Vaccines—Draft. 2022. Available online: https://www.uspnf.com/sites/default/files/uspnf_pdf/EN/USPNF/uspnf-notices/mrna-vaccine-chapter.pdf (accessed on 8 April 2024).

22. WHO. Evaluation of the Quality, Safety and Efficacy of Messenger RNA Vaccines for the Prevention of Infectious Diseases: Regulatory Considerations. 2021. Available online: https://cdn.who.int/media/docs/default-source/biologicals/ecbs/post-ecbs-who-regulatory-considerations-document-for-mrna-vaccines---final-version---29-nov-2021_tz.pdf?sfvrsn=8f57a1af_1&download=true (accessed on 8 April 2024).
23. USP. Analytical Procedures for mRNA Vaccine Quality. 2023. Available online: <https://www.usp.org/sites/default/files/usp/document/our-work/biologics/documents/vaccine-mrna-guidelines-2.pdf> (accessed on 8 April 2024).
24. Andries, O.; Mc Cafferty, S.; De Smedt, S.C.; Weiss, R.; Sanders, N.N.; Kitada, T. N(1)-methylpseudouridine-incorporated mRNA outperforms pseudouridine-incorporated mRNA by providing enhanced protein expression and reduced immunogenicity in mammalian cell lines and mice. *J. Control. Release* **2015**, *217*, 337–344. [[CrossRef](#)]
25. Karikó, K.; Buckstein, M.; Ni, H.; Weissman, D. Suppression of RNA recognition by Toll-like receptors: The impact of nucleoside modification and the evolutionary origin of RNA. *Immunity* **2005**, *23*, 165–175. [[CrossRef](#)]
26. Anderson, B.R.; Muramatsu, H.; Jha, B.K.; Silverman, R.H.; Weissman, D.; Karikó, K. Nucleoside modifications in RNA limit activation of 2'-5'-oligoadenylate synthetase and increase resistance to cleavage by RNase L. *Nucleic Acids Res.* **2011**, *39*, 9329–9338. [[CrossRef](#)]
27. Cheng, F.; Wang, Y.; Bai, Y.; Liang, Z.; Mao, Q.; Liu, D.; Wu, X.; Xu, M. Research Advances on the Stability of mRNA Vaccines. *Viruses* **2023**, *15*, 668. [[CrossRef](#)] [[PubMed](#)]
28. Packer, M.; Gyawali, D.; Yerabolu, R.; Schariter, J.; White, P. A novel mechanism for the loss of mRNA activity in lipid nanoparticle delivery systems. *Nat. Commun.* **2021**, *12*, 6777. [[CrossRef](#)]
29. CDE. Technical Guidelines for Pharmaceutical Research of Novel Coronavirus Prevention mRNA Vaccine (Draft Edition). 2020. Available online: <https://www.cde.org.cn/zdyz/domesticinfopage?zdyzIdCODE=9efa70b504dc5c66965001181a49c30b> (accessed on 8 April 2024).
30. WHO. Thermostability of Vaccines. WHO/GPV/98.07. 1998. Available online: https://iris.who.int/bitstream/handle/10665/64980/WHO_GPV_98.07.pdf?sequence=1 (accessed on 10 January 2024).
31. Hornung, V.; Ellegast, J.; Kim, S.; Brzózka, K.; Jung, A.; Kato, H.; Poeck, H.; Akira, S.; Conzelmann, K.K.; Schlee, M.; et al. 5'-Triphosphate RNA is the ligand for RIG-I. *Science* **2006**, *314*, 994–997. [[CrossRef](#)] [[PubMed](#)]
32. Iurescia, S.; Fioretti, D.; Rinaldi, M. The Innate Immune Signalling Pathways: Turning RIG-I Sensor Activation Against Cancer. *Cancers* **2020**, *12*, 3158. [[CrossRef](#)]
33. Reikine, S.; Nguyen, J.B.; Modis, Y. Pattern Recognition and Signaling Mechanisms of RIG-I and MDA5. *Front. Immunol.* **2014**, *5*, 342. [[CrossRef](#)]
34. Kawasaki, T.; Kawai, T. Toll-like receptor signaling pathways. *Front. Immunol.* **2014**, *5*, 461. [[CrossRef](#)] [[PubMed](#)]
35. Niu, D.; Wu, Y.; Lian, J. Circular RNA vaccine in disease prevention and treatment. *Signal Transduct. Target. Ther.* **2023**, *8*, 341. [[CrossRef](#)]
36. Seephetdee, C.; Bhukhai, K.; Buasri, N.; Leelukkanaveera, P.; Lerdwattanasombat, P.; Manopwisedjaroen, S.; Phueakphud, N.; Kuhaudomlarp, S.; Olmedillas, E.; Saphire, E.O.; et al. A circular mRNA vaccine prototype producing VFLIP-X spike confers a broad neutralization of SARS-CoV-2 variants by mouse sera. *Antivir. Res.* **2022**, *204*, 105370. [[CrossRef](#)]
37. Wu, M.Z.; Asahara, H.; Tzertzinis, G.; Roy, B. Synthesis of low immunogenicity RNA with high-temperature in vitro transcription. *RNA* **2020**, *26*, 345–360. [[CrossRef](#)] [[PubMed](#)]
38. Abe, N.; Matsumoto, K.; Nishihara, M.; Nakano, Y.; Shibata, A.; Maruyama, H.; Shuto, S.; Matsuda, A.; Yoshida, M.; Ito, Y.; et al. Rolling Circle Translation of Circular RNA in Living Human Cells. *Sci. Rep.* **2015**, *5*, 16435. [[CrossRef](#)]
39. Panesar, N.; Tolman, K.; Mazuski, J.E. Endotoxin stimulates hepatocyte interleukin-6 production. *J. Surg. Res.* **1999**, *85*, 251–258. [[CrossRef](#)]
40. Poole, J.A.; Gaurav, R.; Schwab, A.; Nelson, A.J.; Gleason, A.; Romberger, D.J.; Wyatt, T.A. Post-endotoxin exposure-induced lung inflammation and resolution consequences beneficially impacted by lung-delivered IL-10 therapy. *Sci. Rep.* **2022**, *12*, 17338. [[CrossRef](#)]
41. Zhang, W.; Shen, X.; Xie, L.; Chu, M.; Ma, Y. MicroRNA-181b regulates endotoxin tolerance by targeting IL-6 in macrophage RAW264.7 cells. *J. Inflamm.* **2015**, *12*, 18. [[CrossRef](#)] [[PubMed](#)]
42. Sartorius, R.; Trovato, M.; Manco, R.; D'Apice, L.; De Berardinis, P. Exploiting viral sensing mediated by Toll-like receptors to design innovative vaccines. *NPJ Vaccines* **2021**, *6*, 127. [[CrossRef](#)]
43. Luo, D.; Wu, Z.; Wang, D.; Zhang, J.; Shao, F.; Wang, S.; Cestellos-Blanco, S.; Xu, D.; Cao, Y. Lateral flow immunoassay for rapid and sensitive detection of dsRNA contaminants in in vitro-transcribed mRNA products. *Mol. Ther. Nucleic Acids* **2023**, *32*, 445–453. [[CrossRef](#)]
44. Svitkin, Y.V.; Cheng, Y.M.; Chakraborty, T.; Presnyak, V.; John, M.; Sonenberg, N. N1-methyl-pseudouridine in mRNA enhances translation through eIF2 α -dependent and independent mechanisms by increasing ribosome density. *Nucleic Acids Res.* **2017**, *45*, 6023–6036. [[CrossRef](#)] [[PubMed](#)]
45. Chen, Y.G.; Chen, R.; Ahmad, S.; Verma, R.; Kasturi, S.P.; Amaya, L.; Broughton, J.P.; Kim, J.; Cadena, C.; Pulendran, B.; et al. N6-Methyladenosine Modification Controls Circular RNA Immunity. *Mol. Cell* **2019**, *76*, 96–109.e9. [[CrossRef](#)] [[PubMed](#)]
46. Chen, Y.G.; Kim, M.V.; Chen, X.; Batista, P.J.; Aoyama, S.; Wilusz, J.E.; Iwasaki, A.; Chang, H.Y. Sensing Self and Foreign Circular RNAs by Intron Identity. *Mol. Cell* **2017**, *67*, 228–238.e5. [[CrossRef](#)] [[PubMed](#)]

47. Li, H.; Peng, K.; Yang, K.; Ma, W.; Qi, S.; Yu, X.; He, J.; Lin, X.; Yu, G. Circular RNA cancer vaccines drive immunity in hard-to-treat malignancies. *Theranostics* **2022**, *12*, 6422–6436. [[CrossRef](#)] [[PubMed](#)]
48. Mei, Y.; Wang, X. RNA modification in mRNA cancer vaccines. *Clin. Exp. Med.* **2023**, *23*, 1917–1931. [[CrossRef](#)] [[PubMed](#)]
49. Zhang, Z.; Ohto, U.; Shibata, T.; Krayukhina, E.; Taoka, M.; Yamauchi, Y.; Tanji, H.; Isobe, T.; Uchiyama, S.; Miyake, K.; et al. Structural Analysis Reveals that Toll-like Receptor 7 Is a Dual Receptor for Guanosine and Single-Stranded RNA. *Immunity* **2016**, *45*, 737–748. [[CrossRef](#)] [[PubMed](#)]
50. Tanji, H.; Ohto, U.; Shibata, T.; Taoka, M.; Yamauchi, Y.; Isobe, T.; Miyake, K.; Shimizu, T. Toll-like receptor 8 senses degradation products of single-stranded RNA. *Nat. Struct. Mol. Biol.* **2015**, *22*, 109–115. [[CrossRef](#)] [[PubMed](#)]
51. Chen, R.; Wang, S.K.; Belk, J.A.; Amaya, L.; Li, Z.; Cardenas, A.; Abe, B.T.; Chen, C.K.; Wender, P.A.; Chang, H.Y. Engineering circular RNA for enhanced protein production. *Nat. Biotechnol.* **2023**, *41*, 262–272. [[CrossRef](#)] [[PubMed](#)]
52. Meyer, K.D.; Saletore, Y.; Zumbo, P.; Elemento, O.; Mason, C.E.; Jaffrey, S.R. Comprehensive analysis of mRNA methylation reveals enrichment in 3' UTRs and near stop codons. *Cell* **2012**, *149*, 1635–1646. [[CrossRef](#)] [[PubMed](#)]
53. Roundtree, I.A.; Evans, M.E.; Pan, T.; He, C. Dynamic RNA Modifications in Gene Expression Regulation. *Cell* **2017**, *169*, 1187–1200. [[CrossRef](#)] [[PubMed](#)]
54. Zhou, C.; Molinie, B.; Daneshvar, K.; Pondick, J.V.; Wang, J.; Van Wittenberghe, N.; Xing, Y.; Giallourakis, C.C.; Mullen, A.C. Genome-Wide Maps of m6A circRNAs Identify Widespread and Cell-Type-Specific Methylation Patterns that Are Distinct from mRNAs. *Cell Rep.* **2017**, *20*, 2262–2276. [[CrossRef](#)]
55. Dominissini, D.; Moshitch-Moshkovitz, S.; Schwartz, S.; Salmon-Divon, M.; Ungar, L.; Osenberg, S.; Cesarkas, K.; Jacob-Hirsch, J.; Amariglio, N.; Kupiec, M.; et al. Topology of the human and mouse m6A RNA methylomes revealed by m6A-seq. *Nature* **2012**, *485*, 201–206. [[CrossRef](#)]

Disclaimer/Publisher's Note: The statements, opinions and data contained in all publications are solely those of the individual author(s) and contributor(s) and not of MDPI and/or the editor(s). MDPI and/or the editor(s) disclaim responsibility for any injury to people or property resulting from any ideas, methods, instructions or products referred to in the content.